Polar Localization of the Borate Exporter BOR1 Requires AP2-Dependent Endocytosis[1]

Akira Yoshinari,[a,b,2] Takuya Hosokawa,[a] Taro Amano,[b,3] Marcel Pascal Beier,[a] Tadashi Kunieda,[c,d,4] Tomoo Shimada,[d] Ikuko Hara-Nishimura,[c,d] Satoshi Naito,[b,e] and Junpei Takano[a,b,5,6]

[a]Graduate School of Life and Environmental Sciences, Osaka Prefecture University, Sakai 599-8531, Japan
[b]Graduate School of Agriculture, Hokkaido University, Sapporo 060-8589, Japan
[c]Faculty of Science and Engineering, Konan University, Kobe 658-8501, Japan
[d]Graduate School of Science, Kyoto University, Kyoto 606-8502, Japan
[e]Graduate School of Life Science, Hokkaido University, Sapporo 060-0810, Japan

ORCID IDs: 0000-0002-7083-5674 (A.Y.); 0000-0003-4890-2719 (M.P.B.); 0000-0003-1149-7254 (T.K.); 0000-0002-2101-1003 (T.S.); 0000-0001-8814-1593 (I.H.-N.); 0000-0001-7006-5609 (S.N.); 0000-0002-7474-3101 (J.T.).

Boron (B) is an essential element in plants but is toxic when it accumulates to high levels. In root cells of Arabidopsis (*Arabidopsis thaliana*), the borate exporter BOR1 is polarly localized in the plasma membrane toward the stele side for directional transport of B. Upon high-B supply, BOR1 is rapidly internalized and degraded in the vacuole. The polar localization and B-induced vacuolar sorting of BOR1 are mediated by endocytosis from the plasma membrane. To dissect the endocytic pathways mediating the polar localization and vacuolar sorting, we investigated the contribution of the clathrin adaptor protein, ADAPTOR PROTEIN2 (AP2) complex, to BOR1 trafficking. In the mutants lacking μ- or σ-subunits of the AP2 complex, the polar localization and constitutive endocytosis of BOR1 under low-B conditions were dramatically disturbed. A coimmunoprecipitation assay showed association of the AP2 complex with BOR1, while it was independent of YxxΦ sorting motifs, which are in a cytosolic loop of BOR1. A yeast two-hybrid assay supported the interaction of the AP2 complex μ-subunit with the C-terminal tail but not with the YxxΦ motifs in the cytosolic loop of BOR1. Intriguingly, lack of the AP2 subunit did not affect the B-induced rapid internalization/vacuolar sorting of BOR1. Consistent with defects in the polar localization, the AP2 complex mutants showed hypersensitivity to B deficiency. Our results indicate that AP2-dependent endocytosis maintains the polar localization of BOR1 to support plant growth under low-B conditions, whereas the B-induced vacuolar sorting of BOR1 is mediated through an AP2-independent endocytic pathway.

Boron (B) in plant tissues is utilized for the cross-linking of cell wall pectins (Funakawa and Miwa, 2015). Translocation of B from roots to shoots in Arabidopsis (*Arabidopsis thaliana*) requires the borate efflux transporter BOR1 (Takano et al., 2002; Yoshinari and Takano, 2017). BOR1 is localized in the plasma membrane in a polar manner toward the stele side of the root cells to facilitate directional B transport toward the xylem (Takano et al., 2010). BOR1 is constitutively internalized and recycled between the plasma membrane and trans-Golgi network/early endosome (TGN/EE) under low-B conditions (Takano et al., 2005; Viotti et al., 2010; Yoshinari et al., 2018). To avoid overaccumulation of boric acid, which exhibits cytotoxicity at high concentrations, de novo protein synthesis of BOR1 is repressed under high-B conditions (Aibara et al., 2018). In addition, BOR1 accumulated in the plasma membrane is rapidly ubiquitinated and transported to multivesicular bodies/late endosomes (MVBs/LEs) and then to the vacuole for degradation (Takano et al., 2005; Viotti et al., 2010; Kasai et al., 2011). Importantly, both the polar localization and the B-induced rapid degradation of BOR1 require endocytosis mediated by DYNAMIN-RELATED PROTEIN1A (DRP1A), which functions in vesicle scission during clathrin-mediated endocytosis (CME; Fujimoto et al., 2010; Yoshinari et al., 2016).

Endocytosis is the central mechanism to internalize proteins from the plasma membrane to intracellular membrane compartments. CME is the most studied

[1]This work was supported by Research Fellowships for Young Scientists (252799 to A.Y.) and Grants-in-Aid for Young Scientists (A) (26712007 to J.T.) from the Japan Society for the Promotion of Science and by a research grant from the Naito Foundation (to J.T.).

[2]Present address: Institute of Transformative Bio-Molecules, Nagoya University, Nagoya 464-8601, Japan.

[3]Present address: Nissin Foods Holdings Co., Ltd., Tokyo 160-8524, Japan.

[4]Present address: Nara Institute of Science and Technology, 8916-5 Takayama, Ikoma 630-0192, Japan.

[5]Author for contact: jtakano@plant.osakafu-u.ac.jp.

[6]Senior author.

The author responsible for distribution of materials integral to the findings presented in this article in accordance with the policy described in the Instructions for Authors (www.plantphysiol.org) is: Junpei Takano (jtakano@plant.osakafu-u.ac.jp).

A.Y. designed and performed most of the experiments and wrote the article; T.H., T.A., and T.K. performed experiments; T.S. and I.H.-N. supervised the experiments; S.N. supervised the project and complemented the writing; M.P.B. performed experiments and edited the article; J.T. conceived the project and wrote the article with contributions of all the authors.

www.plantphysiol.org/cgi/doi/10.1104/pp.18.01017

endocytic pathway in plants. Clathrin cages the vesicles, forming so-called clathrin-coated vesicles (CCVs), at the plasma membrane and TGN/EEs in plant cells (Dhonukshe et al., 2006; Ito et al., 2012). During CCV formation, adaptor proteins play roles in the initiation of CME through lipid binding, cargo selection, and recruitment of scaffold proteins and clathrins (Kaksonen and Roux, 2018). In plants, the heterooctameric TPLATE complex functions as an early adaptor module, and the classical heterotetrameric ADAPTOR PROTEIN2 (AP2) complex functions as a clathrin adaptor for CME (Gadeyne et al., 2014; Luschnig and Vert, 2014). In addition to AP2, plants have AP1, AP3, AP4, and putative AP5 complexes. AP1 has been shown to be involved in the membrane trafficking from TGN/EE to the plasma membrane and to the vacuole (Park et al., 2013; Sauer et al., 2013; Teh et al., 2013; Wang et al., 2013; Richter et al., 2014). The γ-subunit of AP1 interacts with the [D/E]xxxL[L/I] motif (D/E, Asp or Glu; x, any residues; L, Leu; L/I, Leu or Ile) of the VACUOLAR ION TRANSPORTER1, which is targeted to the tonoplast in Arabidopsis (Wang et al., 2014). AP3 and AP4 have been shown to function also in protein sorting to the vacuole via different pathways (Feraru et al., 2010; Zwiewka et al., 2011; Fuji et al., 2016). The μ-subunit of AP4 interacts with the VACUOLAR SORTING RECEPTOR1 in a YxxΦ motif (Y, Tyr; x, any amino acid residues; Φ, bulky hydrophobic amino acid residues)-dependent manner. Both AP1 and AP4 are localized in the TGN/EE, but they are distributed to distinct subdomains (Fuji et al., 2016).

AP2 consists of the two large subunits, AP2A (α) and AP1/2B (β), a medium subunit, AP2M (μ2), and a small subunit, AP2S (σ2; Traub, 2009; Yamaoka et al., 2013). In mammals, AP2 is essential for early embryonic development but not for cell viability (Motley et al., 2003; Mitsunari et al., 2005). In contrast, lack of a subunit of AP2 does not show lethality in Arabidopsis as well as in *Caenorhabditis elegans* (Bashline et al., 2013; Fan et al., 2013; Gu et al., 2013; Kim et al., 2013; Yamaoka et al., 2013). In Arabidopsis plants lacking a single subunit of AP2, endocytosis of FM4-64, an endocytic tracer, was substantially reduced (Bashline et al., 2013; Fan et al., 2013). Mutants of *AP2M* showed defects in floral organ development such as short stamen filaments, which resulted in low fertility (Kim et al., 2013; Yamaoka et al., 2013). In a mutant of *AP2S*, the formation of clathrin-coated pits was still observed by variable-angle epifluorescence microscopy, although the number of clathrin-coated pits was significantly decreased (Fan et al., 2013).

In Arabidopsis, many plasma membrane proteins have been identified as cargo of the AP2-dependent CME pathway. The auxin efflux transporters PIN1 and PIN2 showed reduced endocytic rates in mutants of *AP2S* and *AP2M*, respectively (Fan et al., 2013; Kim et al., 2013). In these mutants, PIN1 and PIN2 showed ectopic subcellular localizations in embryonic cells and anther filaments, while the localizations in root tip cells were apparently normal (Fan et al., 2013; Wang et al., 2013). Endocytosis of the brassinosteroid receptor BRI1 was also compromised by the knockdown or dominant-negative interference of AP2 subunits (Di Rubbo et al., 2013). The endocytosis rate of the fluorescent brassinosteroid analog AFCS and the phosphorylation of BES1 through BRI1 were decreased by the dominant-negative interference of AP2 (Di Rubbo et al., 2013). Endocytosis of the boric acid channel NIP5;1 was also shown to require AP2. In the *ap2m-1* and *ap2m-2* mutants, polar localization of NIP5;1 in root epidermal cells was abolished (Wang et al., 2017). Thus, AP2-dependent CME plays an important role in the internalization of various plasma membrane proteins. In mammalian cells, the μ-subunit of AP2 binds the YxxΦ motif for endocytic cargo selection (Ohno et al., 1995). Consistently, Arabidopsis AP2M can bind to YxxΦ motifs of an *Agrobacterium tumefaciens*-derived virulence protein, VirE2, and the AP2M-VirE2 interaction facilitates internalization of VirE2 and efficient *A. tumefaciens* infection (Li and Pan, 2017). Among endogenous plasma membrane proteins, the cytosolic loop of PIN1 was shown to bind to AP2M in a YxxΦ motif-dependent manner (Sancho-Andrés et al., 2016). However, trafficking and localization of PIN1-GFP was not altered by mutations in the Tyr residues. Therefore, the mechanisms underlying endocytic cargo selection by AP2 remain to be elucidated in plant cells.

BOR1 contains YxxΦ motifs (Y_{373}QLL, Y_{398}DNM, and Y_{405}HHM) within its cytosolic large loop between the 10th and 11th transmembrane domains (Takano et al., 2010; Thurtle-Schmidt and Stroud, 2016). Mutations in these Tyr residues inhibited the polar localization and B-induced vacuolar sorting of BOR1 (Takano et al., 2010). In addition, a chimera analysis with the homolog BOR4 showed that a latter half of the C-terminal cytosolic tail (F642–N704) of BOR1 is required for the polar localization toward the stele side but not for the B-induced rapid degradation (Kasai et al., 2011). This sequence is possibly recognized by AP complexes for the endocytosis and the intracellular trafficking of BOR1.

In this study, we investigated the contribution of AP2 to the polar localization and vacuolar sorting of BOR1 in Arabidopsis. Our results indicate that plants have AP2-dependent and AP2-independent endocytic pathways, which are involved in polar localization and vacuolar sorting of BOR1, respectively.

RESULTS

Polar Localization of BOR1 Is Maintained by AP2-Dependent Endocytosis

We previously demonstrated that polar localization of BOR1 requires DRP1-dependent vesicle scission (Yoshinari et al., 2016). Here, we investigated whether AP2, which is considered to play roles in cargo selection and clathrin recruitment in the plasma membrane, is involved in the polar localization of BOR1. For this

purpose, we analyzed the subcellular localization of BOR1-GFP expressed under the control of the native promoter in mutants lacking the μ-subunit (AP2M) or the σ-subunit (AP2S). To examine the polar localization, confocal images were taken at the root tip center, where all cell layers are represented (Fig. 1A). BOR1-GFP was localized in the plasma membrane with stele-side polarity in the primary root tip cells of wild-type plants, while the polar localization was disturbed in *ap2m-1*, *ap2m-2*, and *ap2s* mutants (Fig. 1A). We calculated polarity indexes of BOR1-GFP in the epidermal cells in the meristematic and transition zones of the roots (Fig. 1B). The polarity index of BOR1-GFP in the wild type (a functionally complemented *bor1-1* line; Takano et al., 2010) was 1.94 $\pm$ 0.46 (mean $\pm$ SD), whereas those of *ap2m-1*, *ap2m-2*, and *ap2s* were significantly decreased to 1.05 $\pm$ 0.25, 0.86 $\pm$ 0.16, and 0.81 $\pm$ 0.14, respectively. These results indicate the importance of AP2-dependent endocytosis for the maintenance of the polar localization of BOR1. We also noticed irregular and swollen cell shapes in the root tip of the *ap2* mutants (Fig. 1A). Intriguingly, in the endodermal cells of the mature portion of roots in the *ap2* mutants, BOR1-GFP retained stele-side polarity (Fig. 1C). This is probably due to the polar exocytosis and the presence of the Casparian strip domain functioning as a membrane diffusion barrier (Alassimone et al., 2010).

Next, we compared the subcellular localization of BOR1-GFP in the cotyledon epidermis of *ap2m-2* and *ap2s* with that of wild-type plants. In the wild-type background, BOR1-GFP showed polar localization toward the inner side of the cotyledon, as we have shown previously (Yoshinari et al., 2016). However, the polar localization of BOR1-GFP was abolished in the *ap2* mutants (Fig. 1D). We also noticed abnormal invaginations of the plasma membrane using BOR1-GFP as a plasma membrane marker in the leaf epidermal cells of *ap2* mutants (Supplemental Fig. S1). This morphological change is comparable to that in the leaf pavement cells of the *stomatal cytokinesis defective2* mutant, in which endocytosis is compromised (McMichael et al., 2013). We also analyzed the subcellular localization of BOR2, the closest homolog of BOR1 (Miwa et al., 2013), in the root of the *ap2s* mutant. In the epidermal cells of *ap2s*, the stele-side polar localization of BOR2-GFP was disturbed (Supplemental Fig. S2A). In contrast, PIN2-GFP showed apical polar localization in the root epidermal cells of *ap2m-1* and *ap2m-2*, as previously reported (Supplemental Fig. S2B; Wang et al., 2016). This observation was supported by immunofluorescence analysis using an anti-PIN2 antibody. Even in the root epidermal cells in which polar localization of BOR1-GFP was abolished, PIN2 proteins were preferentially localized in the apical plasma membrane domains (Supplemental Fig. S2C). These results suggest that the polar localization of BOR1 and BOR2 toward stele and the polar localization of PIN2 toward apical sides are maintained at least partially by distinct mechanisms.

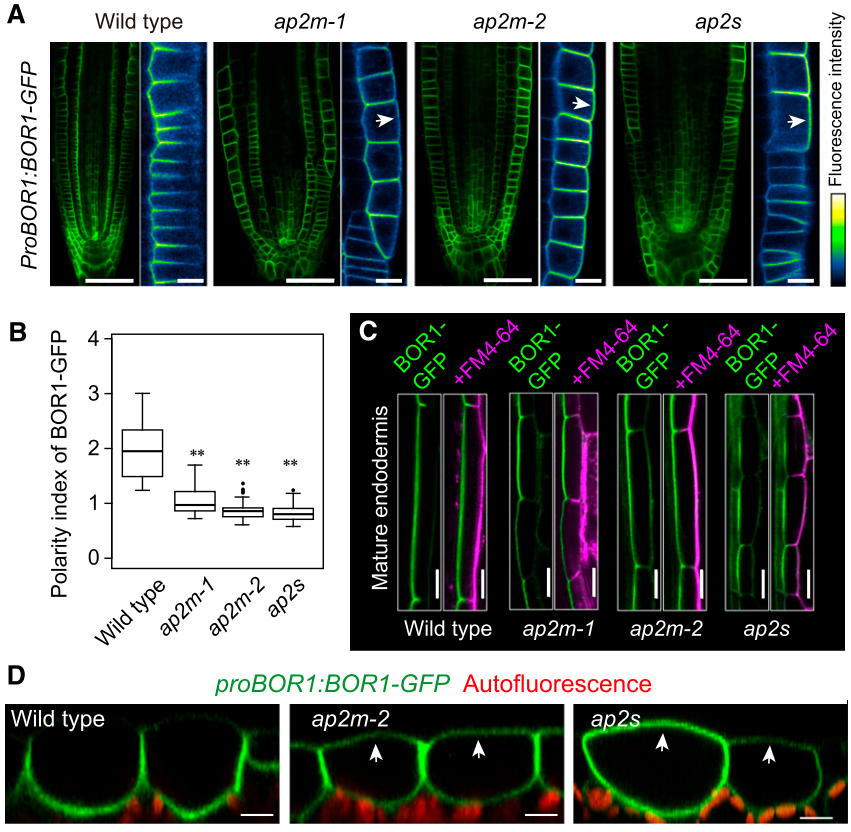

Figure 1. AP2-dependent endocytosis maintains polar localization of BOR1. A, BOR1-GFP in root tips of wild-type (*bor1-1*), *ap2m-1*, *ap2m-2*, and *ap2s* plants. BOR1-GFP in epidermal cell layers is color coded from black to white. Arrows indicate ectopic localization of BOR1-GFP in the outer plasma membrane domains. B, Polarity indexes of BOR1-GFP in epidermal cells in root meristematic zone and transition zone in wild-type (*bor1-1*), *ap2m-1*, *ap2m-2*, and *ap2s* plants. Box plots show the distribution among 50 (wild type), 53 (*ap2m-1*), 43 (*ap2m-2*), and 45 (*ap2s*) cells from three or four independent primary roots. The first and third quartiles and median (line in the box) with whiskers extending to 1.5 $\times$ interquartile range beyond the box are shown. Outliers are displayed by dots. Asterisks indicate significant differences compared with the wild type (**, $P < 0.0001$ by two-tailed Student's *t*-test). C, BOR1-GFP in mature endodermal cells. The roots were incubated with FM4-64 for 20 min. FM4-64 stained outer (soil-side) plasma membrane domains but not inner (stele-side) domains because of the Casparian strip, which functions as an apoplastic and membrane diffusion barrier (Alassimone et al., 2010). D, BOR1-GFP in cotyledon epidermal cells of wild-type (*bor1-1*), *ap2m-2*, and *ap2s* plants. Arrows indicate localization of BOR1-GFP. Bars = 50 μm (A, root tips), 10 μm (A, enlarged images), 20 μm (C), and 10 μm (D).

AP2 Is Involved in Constitutive Endocytosis of BOR1

We have previously shown that the polar localization of BOR1-GFP in the root meristematic zone requires the YxxΦ motifs in the large loop at the cytosolic side (Takano et al., 2010). This might be due to recognition of the YxxΦ motifs by the AP2 complex for constitutive endocytosis under low-B conditions. To examine whether AP2 contributes to constitutive endocytosis of BOR1, we analyzed the internalization of BOR1-GFP and the variant that carries triple Y-to-A substitutions (Y373A·Y398A·Y405A) using brefeldin A (BFA; Fig. 2). The confocal images were taken at a position near the cover slips, where the GFP signal is efficiently obtained but the polar localization is not represented (Fig. 2A). BFA is an inhibitor for subsets of ADP-ribosylation factor guanine nucleotide exchange factors and inhibits endocytic recycling of endocytosed cargo in root cells of Arabidopsis. Previous reports demonstrated that BOR1 is actively transported into endosomal aggregates (BFA compartments) derived from the TGN/EE during BFA treatment (Takano et al., 2005, 2010; Yoshinari et al., 2018). As shown in the previous study, BOR1-GFP and the Y373A·Y398A·Y405A variant were similarly internalized and accumulated in the BFA compartments (Fig. 2A; Takano et al., 2010). However, in the *ap2m-2* mutant, internalization of BOR1-GFP was reduced (Fig. 2A). To quantify the internalization rates, we calculated the ratio of the BOR1-GFP fluorescence in the cytoplasm compared with the plasma membrane (Fig. 2B). The ratios were not significantly different between BOR1-GFP and the Y373A·Y398A·Y405A variant before and after the BFA treatment for 60 min in the wild-type background. However, the ratios of the BOR1-GFP were significantly lower in the *ap2m-2* plants than in the wild-type plants before and after the BFA treatment. These results indicate that AP2 plays an important role in the constitutive endocytosis of BOR1, whereas Y373, Y398, and Y405 of BOR1 are not required for this pathway.

To address the physical association between BOR1 and AP2, we performed coimmunoprecipitation (Co-IP) analysis using an anti-AP2A (α-subunit of AP2 complex) antibody. We used BRI1-GFP, an interactor of AP2A (Di Rubbo et al., 2013), as a positive control and free GFP as a negative control. As expected, AP2A was coimmunoprecipitated with BRI1-GFP but not with free GFP (Fig. 3). Intriguingly, AP2A signals were detected in the lanes of both BOR1-GFP and the Y373A·Y398A·Y405A variant (Fig. 3), suggesting that the YxxΦ motifs of BOR1 are not essential for the association with the AP2 complex. To further analyze the function of the YxxΦ motifs, we tested the physical interaction between the large loop of BOR1 containing the YxxΦ motifs (Fig. 4A) and μ-subunits of AP complexes from Arabidopsis by a yeast two-hybrid (Y2H) assay. Strikingly, no interaction was detected with AP1M2 and AP2M, while an interaction was detected with AP3M and AP4M (Fig. 4B). The interactions with AP3M and AP4M were weakened by the

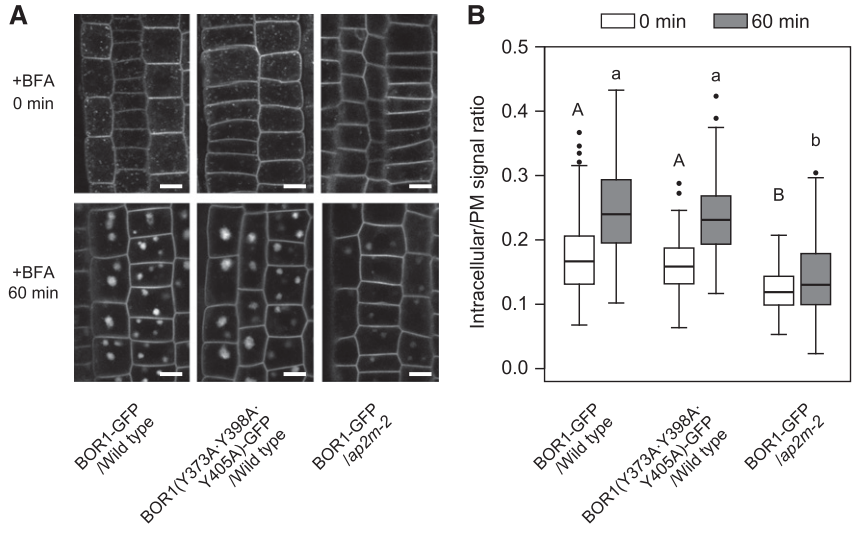

Figure 2. AP2 plays an important role in constitutive endocytosis of BOR1. Plants were treated with 50 μM cycloheximide for 30 min and imaged (0 min) or further treated with 50 μM BFA and 50 μM cycloheximide for 60 min (60 min). A, BOR1-GFP and the Y373A·Y398A·Y405A variant in the root epidermal cells of wild-type (*bor1-1*) or *ap2m-2* plants. The confocal images were taken at a position near the cover slips, where the polar localization is not represented. Bars = 10 μm. B, Fluorescence ratio of GFP in cytoplasm and plasma membrane (PM; cytoplasm/plasma membrane). Box plots show the distribution among 154 (BOR1-GFP/wild type, 0 min), 122 (BOR1-GFP/wild type, 60 min), 150 (Y373A·Y398A·Y405A/wild type, 0 min), 218 (Y373A·Y398A·Y405A/wild type, 60 min), 75 (BOR1-GFP/*ap2m-2*, 0 min), and 92 (BOR1-GFP/*ap2m-2*, 60 min) cells from three or four independent primary roots. The first and third quartiles and median (line in the box) with whiskers extending to 1.5 × interquartile range beyond the box are shown. Outliers are displayed by dots. Letters above the whiskers represent statistical significance (one-way ANOVA with Steel-Dwass posthoc test, $P < 0.0001$).

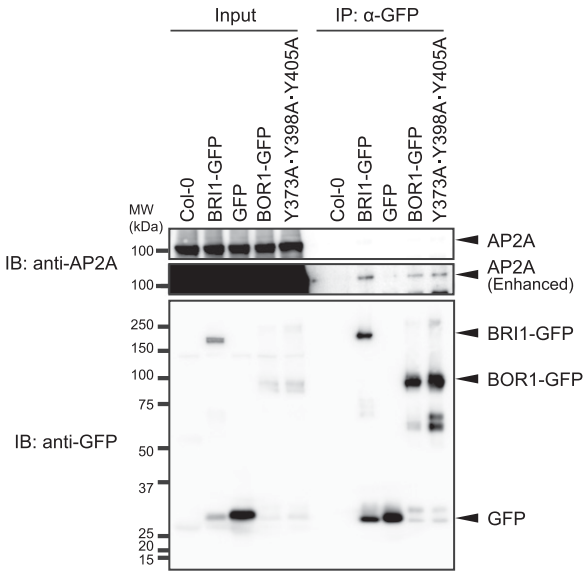

Figure 3. BOR1 is associated with the AP2 complex in a YxxΦ motif-independent manner. Co-IP analysis is shown for BOR1-GFP and AP2A. BRI1-GFP, free GFP, BOR1-GFP, and BOR1(Y373A·Y398A·Y405A)-GFP were immunoprecipitated using anti-GFP magnetic beads and detected by anti-AP2A (top and middle) and anti-GFP (bottom) antibodies. Protein molecular masses of AP2A, BRI1-GFP, BOR1-GFP, and free GFP are predicted to be 112, 158, 106, and 27 kD, respectively. Col-0, Columbia-0; IB, immunoblotting; IP, immunoprecipitation.

Y373A·Y398A·Y405A substitution. The Arabidopsis AP2M and AP1M2 constructs showed interactions with the N-terminal domain of human transferrin receptor (TfR; Supplemental Fig. S3), which is a cargo of AP2-dependent CME in human cells (Motley et al., 2003), suggesting that these constructs are functional. Taken together, these results suggest that the YxxΦ motifs of BOR1 are not involved in AP2-dependent endocytosis but are involved in AP3- and AP4-mediated vesicle transport. We then tested the interaction with the latter half of the C-terminal cytosolic tail (R637–N704) of BOR1, a region previously shown to be required for the polar localization toward the stele side but not for B-induced rapid degradation (Kasai et al., 2011; Fig. 4A). Strikingly, an interaction was detected with AP2M but not with AP1M2, AP3M, and AP4M (Fig. 4C), suggesting that the C-terminal tail is involved in AP2-dependent endocytosis.

B-Induced Degradation of BOR1 Is Independent of AP2-Mediated Endocytosis

To test whether AP2 is involved in B-induced degradation of BOR1, we performed time-course confocal imaging of the root epidermal cells in wild-type, *ap2m-1*, and *ap2m-2* plants (Fig. 5). To assess the effects of B-dependent translational repression (Aibara et al., 2018) and photobleaching due to long observation times, we also observed BOR1(K590A)-GFP, a variant of BOR1-GFP lacking its ubiquitination site (Kasai et al., 2011), expressed under the control of the BOR1 promoter. After high-B supply, BOR1-GFP in the wild-type background showed rapid internalization and the fluorescence levels in the plasma membrane decreased to ~10% within 120 min, while BOR1(K590A)-GFP showed stable accumulation in the plasma membrane (Fig. 5, A and B). Surprisingly, in the mutants lacking *AP2M*, BOR1-GFP showed rapid internalization and decrease of fluorescence intensity in the plasma membrane, similar to the case in the wild-type background (Fig. 5, A and B). Consistently, western-blot analysis detecting endogenous BOR1 protein in the root tissue using a BOR1-specific antibody (Supplemental Fig. S4) showed a similar decrease of BOR1 protein levels in wild-type and *ap2m-2* mutant plants after high-B supply (Fig. 5C). Thus, although constitutive endocytosis of BOR1 was largely dependent on the AP2-mediated pathway, B-induced rapid internalization of BOR1 was not impaired in the *ap2m* mutants. These results suggest that AP2-dependent and -independent pathways distinctly contribute to the internalization of BOR1 for different destinations.

AP2 Is Essential for Plant Growth under B-Deficient Conditions

We demonstrated that AP2-dependent endocytosis is required for polar localizations of B transporters including BOR1 (Fig. 1), BOR2 (Supplemental Fig. S2), and NIP5;1 (Wang et al., 2017). The polar localizations of B transporters are considered essential for directional transport of boric acid from distal to proximal cell layers (Yoshinari and Takano, 2017). Therefore, we investigated the growth of the *ap2m* mutants under low- to sufficient-B conditions. Under 0.01 μM boric acid, the *ap2m* mutants showed more severe growth reduction of the whole plant than the wild-type plants (Fig. 6A). Apparently, the growth defects of the *ap2m* mutants were alleviated by elevation of the boric acid concentration to a sufficient level, with the growths becoming similar under 30 μM boric acid (Fig. 6, A and B). To compare the susceptibility to B deficiency, we calculated the ratio of primary root length under 0.01 to 30 μM boric acid conditions. The ratios in the *ap2m* mutants were significantly lower than in the wild-type plants (Fig. 6C), indicating a higher susceptibility to B deficiency. A similar growth reduction under a B-deficient condition was observed in the *ap2s* mutant (Supplemental Fig. S5). To further analyze the effects of B deficiency on the *ap2m* mutants, we compared the morphology of 10-d-old seedlings of the wild type, *ap2m-1*, *ap2m-2*, and the *bor1-3 bor2-1* double mutant (Kasai et al., 2011). All the plants showed similar morphology under sufficient-B conditions (30 μM; Fig. 6D). Intriguingly, both the *ap2m* mutants and the *bor1-3 bor2-1* double mutant showed reduced expansion of the cotyledons, no appearance of true leaves, and swelling of the root tip (Fig. 6E). These results demonstrate the

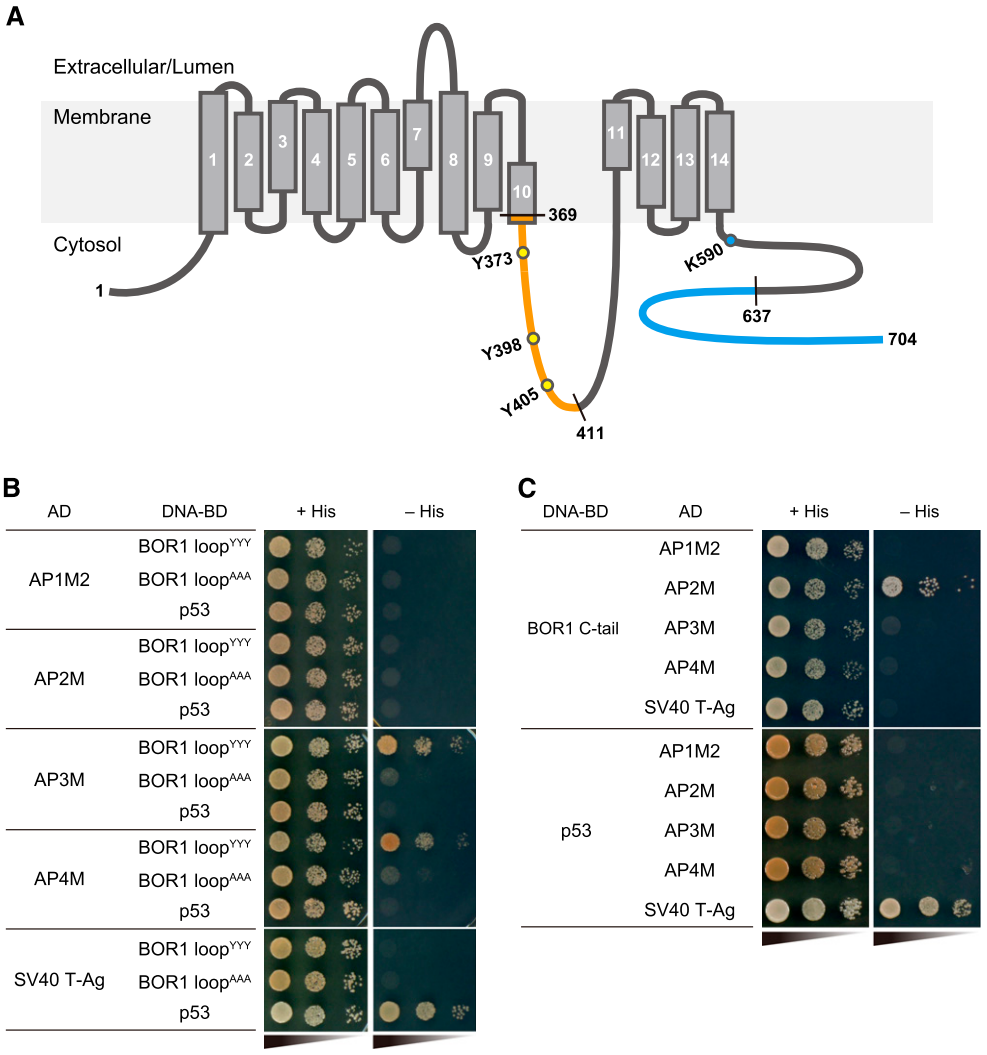

Figure 4. Interaction between BOR1 and μ-subunits of AP complexes. A, Topological model of Arabidopsis BOR1 (Thurtle-Schmidt and Stroud, 2016). Orange and blue lines indicate regions used in Y2H analysis. Black and white numbers/letters indicate amino acid positions and transmembrane helix numbers, respectively. B and C, Y2H analysis between the BOR1 large loop (369–411; B) or C tail (637–704; C) and the μ-subunits of four AP complexes (AP1, AP2, AP3, and AP4). Combination of SV40 T-antigen and p53 was used as a positive control. A His biosynthesis gene was used as a reporter for the interaction in an auxotroph yeast strain. AAA, Mutated BOR1 large loop with Y373A·Y398A·Y405A substitutions; AD, prey constructs fused with the GAL4 activation domains; DNA-BD, bait constructs fused with the GAL4 DNA-binding domains; YYY, wild-type BOR1 large loop.

importance of the AP2-mediated endocytosis for plant growth under low-B conditions.

DISCUSSION

Previously, we reported that both polar localization toward the stele side and B-induced vacuolar sorting of BOR1 depend on DRP1-mediated endocytosis in Arabidopsis (Yoshinari et al., 2016). However, it was unclear whether the endocytic mechanisms leading to the different destinations are the same or not. In this study, we showed that the AP2 complex is required for the constitutive endocytosis mediating polar localization but not for the inducible endocytosis that leads to the vacuolar sorting of BOR1.

AP2 Is Required for Constitutive Endocytosis and Polar Localization of BOR1

In the root tip of mutants lacking AP2M or AP2S, the polar localization of BOR1-GFP was impaired (Fig. 1) and constitutive endocytosis visualized by a BFA treatment was decreased (Fig. 2). These results were similar to our previous observation, which showed that the polar localization toward the soil side and the endocytosis of GFP-NIP5;1 were impaired in mutants lacking AP2M (Wang et al., 2017). In the plasma membrane, BOR1, NIP5;1, and other multispanning membrane proteins showed substantial lateral diffusion, although the rate was much slower than in the plasma membrane of animal cells (Takano et al., 2010; Martinière et al., 2012; Hosy et al., 2015; Yoshinari et al., 2016). Therefore, our results suggest that the constitutive endocytosis mediated by AP2 and the subsequent recycling are important factors for the maintenance of the polar localization of transport proteins toward the stele and soil sides in the plasma membrane without diffusion barrier. Intriguingly, the stele-side polarity of BOR1-GFP was still maintained in the mature endodermal cells of the *ap2* mutants (Fig. 1). This can be interpreted that once the polar localization is established by a polar exocytosis, constitutive endocytosis is not required for the maintenance of the polar

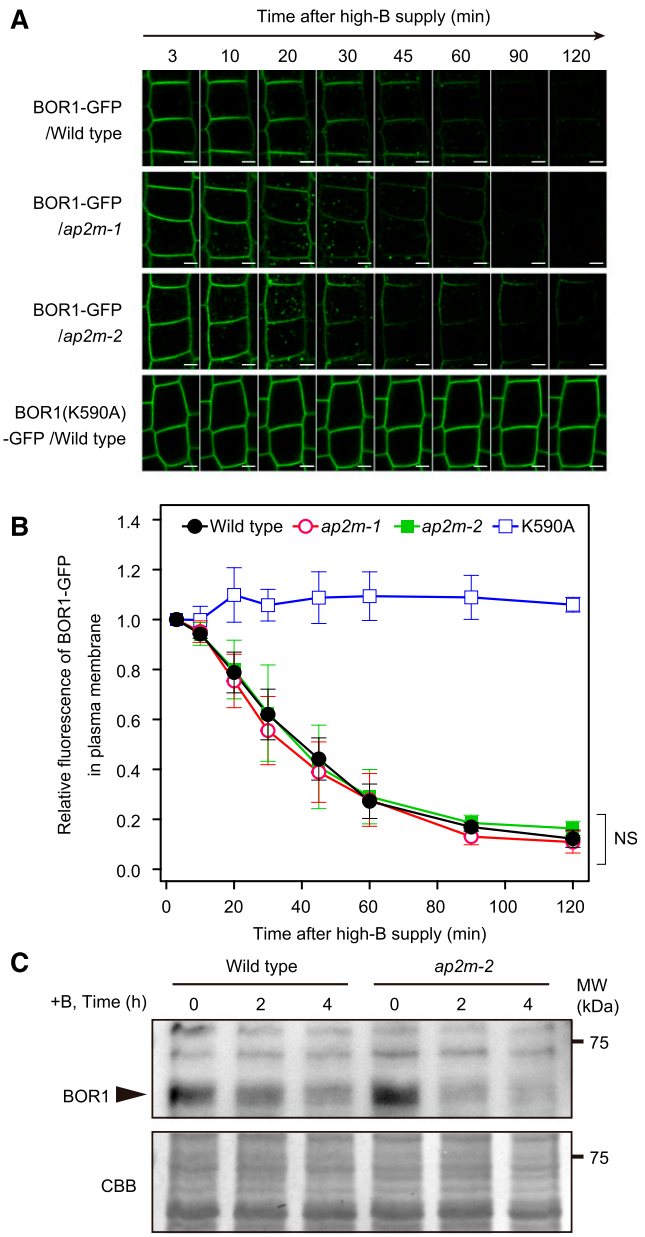

Figure 5. B-dependent rapid internalization of BOR1 does not require AP2 function. Time-course analyses are shown for BOR1-GFP and the K590A variant in wild-type (*bor1-1*) or *ap2m* plants. The transgenic plants were grown on low-B (0.5 μM) medium for 4 d and then shifted to high-B (100 μM) medium. A, Time-course imaging in root epidermal cells. The confocal images were taken at a position near the cover slips, where the polar localization is not represented. Bars = 5 μm. B, Relative GFP fluorescence levels in the plasma membrane of epidermal cells. The values were normalized by those at 3 min after the shift to 100 μM B medium. Bars represent means ± SD. n = 6 (wild type; 207 cells), 4 (*ap2m-1*; 129 cells), 3 (*ap2m-2*; 88 cells), and 3 (K590A; 81 cells) independent roots. Differences among the wild type, *ap2m-1*, and *ap2m-2* were determined by two-way ANOVA (NS, no significant difference [$P > 0.5$]). C, Western-blot analysis of endogenous BOR1 in roots. Endogenous BOR1 protein showed similar migration to that of ~63-kD proteins (Supplemental Fig. S5). CBB, Coomassie Brilliant Blue staining for loading control.

localization in the mature endodermal cells, because the Casparian strip domain prevents the lateral diffusion of BOR1 in the plasma membrane (Alassimone et al., 2010; Takano et al., 2010).

Previously, the YxxΦ motifs in the large loop of BOR1 were shown to be required for polar localization (Takano et al., 2010). In this study, we investigated the possible requirement of the YxxΦ motifs in AP2-mediated endocytosis. However, BOR1(Y373A·Y398A·Y405A)-GFP was accumulated in BFA compartments in the same manner as the wild-type BOR1-GFP, indicating that the YxxΦ motifs are not involved in the constitutive endocytosis of BOR1 (Fig. 2). Consistently, the Co-IP analysis indicated that the YxxΦ motifs of BOR1 are not involved in the association with the AP2 complex (Fig. 3). In addition, the Y2H analysis indicated that AP2M does not interact with the large loop containing the YxxΦ motifs but with the C-terminal tail of BOR1 (Fig. 4). Future analysis of the in vivo interaction by a method such as Förster resonance energy transfer-fluorescence lifetime imaging microscopy would provide us with spatiotemporal information of the interaction between BOR1 and the AP2 complex at specific membrane domains.

Taken together, we conclude that the polar localization of BOR1 is maintained by AP2-dependent endocytosis, which is independent of the YxxΦ motifs (Fig. 7A). It is likely that the YxxΦ motifs are directly or indirectly involved in an unknown polar-exocytosis pathway (Fig. 7B).

B-Induced Vacuolar Sorting Depends on AP2-Independent Endocytosis

In this study, we showed that constitutive endocytosis and the polar localization of BOR1 were impaired, while B-induced internalization and vacuolar sorting of BOR1 were not influenced in mutants lacking AP2M or AP2S (Figs. 1, 2, and 5). We also showed that AP2M binds to the latter half of the BOR1 C-terminal tail (637–704; Fig. 4C), corresponding to the region required for the polar localization but not for the B-induced degradation (Kasai et al., 2011). These results suggest that recognition of the C-terminal tail by the AP2 complex initiates endocytosis of BOR1 for maintenance of the polar localization but not for degradation (Fig. 7A). Previously, we have demonstrated that DRP1 is essential for both the polar localization and the B-induced internalization and vacuolar sorting of BOR1 (Yoshinari et al., 2016; Fig. 7, A and C). These findings suggest that DRP1-dependent but AP2-independent endocytosis leads to B-induced internalization and vacuolar sorting of BOR1 (Fig. 7C). Under high-B conditions, ubiquitination of BOR1 at K590 located at the beginning of the C-terminal cytosolic tail (predicted to start from F588) is required for vacuolar targeting (Kasai et al., 2011). The ubiquitinated BOR1 is possibly recognized by ubiquitin-binding proteins, such as TOM1-LIKEs (TOLs) and Src homology-3 domain-containing protein2 (SH3P2), at the plasma membrane

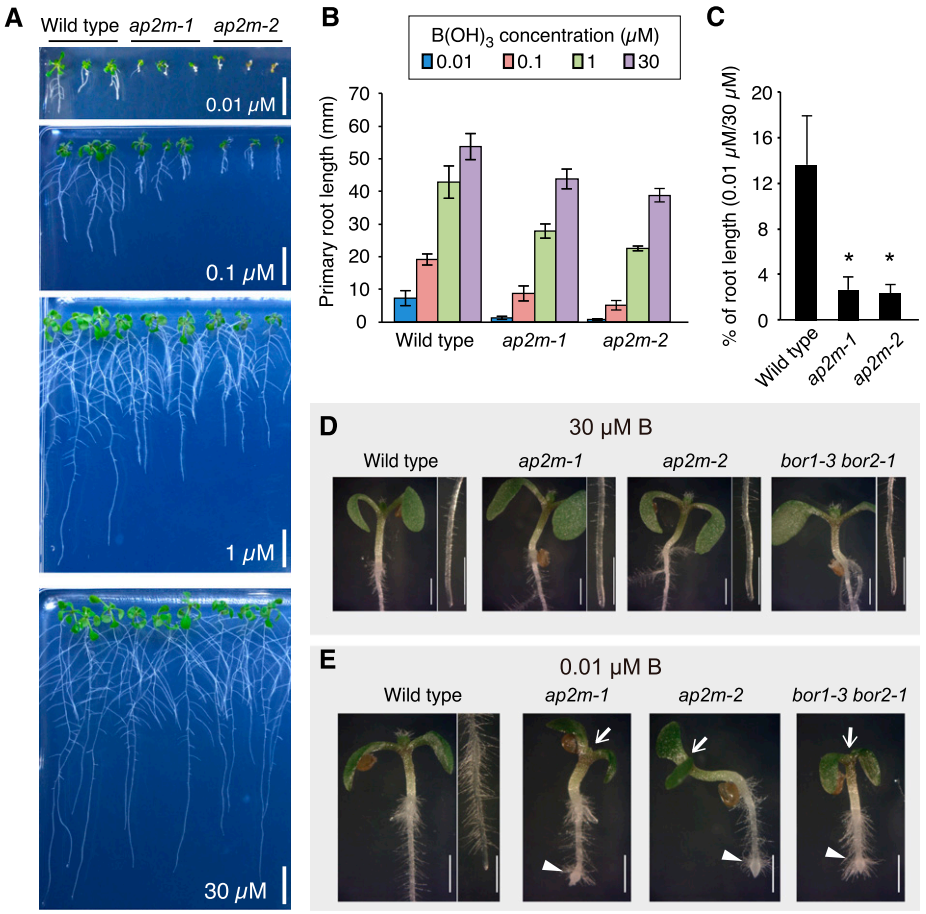

Figure 6. AP2-dependent endocytosis is essential for plant growth under B-deficient conditions. A, Ten-day-old wild-type Col-0, *ap2m-1*, and *ap2m-2* plants grown with 0.01, 0.1, 1, or 30 μM boric acid. Bars = 10 mm. B, Primary root lengths. $n = 5$ to 9 seedlings. Bars represent means ± SD. C, Relative root lengths at 0.01 μM B compared with those at 30 μM B condition. Bars represent means ± SD. Asterisks indicate $P <$ 0.0001 determined by Student's *t* test. D and E, Stereomicroscopic images of 5-d-old seedlings of wild-type (Col-0), *ap2m-1*, *ap2m-2*, and *bor1-3 bor2-1* grown with 30 μM (D) or 0.01 μM (E) boric acid. Arrows indicate impaired expansion of true leaves, and arrowheads indicate swelling of roots. Bars = 1 mm.

(Korbei et al., 2013; Nagel et al., 2017). Subsets of TOL family proteins are likely localized in the plasma membrane for the early recognition and sequestration of ubiquitinated cargo for the endosomal sorting complex required for transport (ESCRT) machinery (Korbei et al., 2013; Fig. 7D). Indeed, a recent study revealed that a quintuple knockout of *TOL* genes (*tol23569*) dramatically inhibits vacuolar sorting of BOR1 under a high-B condition (Yoshinari et al., 2018). SH3P2 also binds to ubiquitinated cargoes directly and functions together with ESCRT-I (Nagel et al., 2017). Intriguingly, both TOL and SH3P2 proteins are suggested to associate with clathrin. Six of the nine TOLs were predicted to have clathrin-binding motifs (Korbei et al., 2013), and SH3P2 was cofractionated with CCVs (Nagel et al., 2017). Therefore, either or both protein families possibly mediate loading of the ubiquitinated BOR1 proteins into CCVs in an AP2-independent manner.

The YxxΦ motifs of BOR1 are also involved in the B-dependent vacuolar targeting but not in the constitutive endocytosis (Fig. 2; Takano et al., 2010; Yoshinari et al., 2012). The Y2H analysis suggested that the YxxΦ motifs of BOR1 potentially bind to the μ-subunits of AP3 and AP4 complexes (Fig. 4B). In plant cells, AP3 is involved in vacuolar protein sorting and vacuolar function (Feraru et al., 2010; Zwiewka et al., 2011; Wolfenstetter et al., 2012). AP4 is involved in the vacuolar protein sorting of VACUOLAR SORTING RECEPTOR1 in a YxxΦ(E) motif-dependent manner in Arabidopsis (Fuji et al., 2016). It is possible that AP3 and/or AP4 function in vacuolar sorting of BOR1 from TGN or other post-Golgi compartments by recognizing the YxxΦ motifs (Fig. 7E). Further analysis is required to elucidate this pathway.

AP2 Is Essential for Plant Growth under B-Deficient Conditions

Under low-B conditions, plants utilize B transporters, which are polarly localized in the plasma membrane in root tissue. NIP5;1 is located in the soil-side domain and BOR1/BOR2 is located in the stele-side domain of the plasma membrane. They cooperatively facilitate the transport of boric acid from soil to stele (Yoshinari and Takano, 2017). Previously, we reported that a GFP-NIP5;1 variant lacking specific phosphorylation sites, which are required for the constitutive endocytosis and polar localization but not for the transport activity, only partially complements the defective growth of the *nip5;1* loss-of-function mutant (Wang et al., 2017). This result demonstrated the importance of the polar localization of NIP5;1 for efficient B transport. In this study, we analyzed the phenotype of AP2 mutants in which

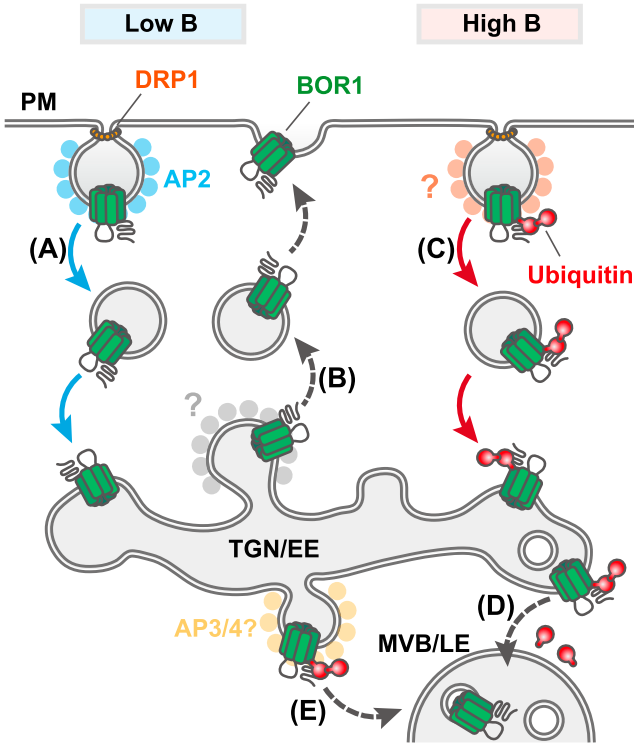

Figure 7. Schematic model of endocytosis and intracellular trafficking of BOR1. A, Under low-B conditions, BOR1 is internalized via AP2- and DRP1-dependent endocytosis. This endocytic pathway plays an important role for maintenance of the polar localization of BOR1 and does not rely on the YxxΦ motifs of BOR1. B, The YxxΦ motifs of BOR1 are involved in polar recycling of BOR1 to a specific plasma membrane domain by an unknown mechanism. C, Under high-B conditions, BOR1 undergoes ubiquitination. The ubiquitinated BOR1 is internalized via AP2-independent but DRP1-dependent endocytosis. D, The ubiquitinated BOR1 is transported into intralumenal vesicles of MVB/LE through TOL proteins and the ESCRT machinery. E, The YxxΦ motifs of BOR1 potentially interact with AP3M and AP4M and for B-induced degradation of BOR1. The ubiquitinated BOR1 may be transported to MVB/LE via AP3/4-dependent vesicle trafficking.

the polar localization of NIP5;1, BOR1, and BOR2 is impaired (Fig. 1; Wang et al., 2017). Based on this impairment, a disturbance of the intercellular B transport system is expected. Consistent with previous reports showing severe growth defects only in the reproductive stage (Fan et al., 2013; Kim et al., 2013; Yamaoka et al., 2013; Bashline et al., 2015), the growths of *ap2m* and *ap2s* mutants in the vegetative stage were only moderately reduced under sufficient-B conditions (10 and 30 μM; Fig. 6, A, B, and D; Supplemental Fig. S5). However, under low-B conditions, these mutants showed significant growth reduction (Fig. 6, A–C and E; Supplemental Fig. S5). Especially at severe B limitation (0.01 μM), these mutants showed striking growth defects, such as root swelling and impaired expansion of true leaves, similar to those of the *bor1-3 bor2-1* double knockout mutant (Fig. 6E; Supplemental Fig. S5). These data suggest the physiological significance of AP2 in the efficient uptake and translocation of boric acid under low-B conditions through the maintenance of the lateral polar localization of multiple B transporters.

In summary, our data suggest that the polar localization of BOR1 is maintained through AP2-dependent endocytosis, whereas vacuolar sorting of ubiquitinated BOR1 is mediated through an AP2-independent endocytic pathway. Our data also highlighted the physiological significance of AP2-mediated endocytosis in nutrient transport.

MATERIALS AND METHODS

Plasmid Construction

To construct bait vectors for the Y2H analysis, sequences encoding the large loop (369–411) or C-terminal tail (637–704) of BOR1 and the N-terminal region (1–61) of TfR (GenBank accession no. AF187320.1) were amplified by PCR using specific primers (Supplemental Table S1) from cDNA pools of Arabidopsis (*Arabidopsis thaliana*) Col-0 tissues or human cultured-HaCaT cells and introduced into *Eco*RI/*Bam*HI double-digested pGBKT7 vector by In-Fusion cloning (Takara Clontech). To construct prey vectors for the Y2H analysis, the coding sequences of AP1M2, AP2M, and AP3M were amplified by PCR using specific primers (Supplemental Table S1) and subcloned into the Gateway entry vectors as follows. The AP1M2 sequence was introduced into *Asp*718I-*Not*I double-digested pENTR1A vector by the In-Fusion reaction (Takara Clontech), while the AP2M and AP3M sequences were introduced into pENTR/D-TOPO vector by TOPO cloning (Invitrogen). The resulting entry vectors were transferred into the pDEST-GADT7 vector (Rossignol et al., 2007) by the Gateway LR reaction (Invitrogen). The AP4M prey vector has been reported previously (Fuji et al., 2016).

Plant Materials and Growth Conditions

The Col-0 ecotype of Arabidopsis was from our laboratory stock. The *ap2m-1* (SALK_083693), *ap2m-2* (SAIL_165_A05), *ap2s* (SALK_141555), and *bor1-3 bor2-1* lines were described previously (Kasai et al., 2011; Fan et al., 2013; Kim et al., 2013; Yamaoka et al., 2013). The transgenic plants harboring *ProBOR1:BOR1-GFP* or *ProBOR1:BOR1(Y373A·Y398A·Y405A)-GFP* in the *bor1-1* background and *ProBOR2:BOR2-GFP* in the *bor2-1* background were described previously (Takano et al., 2010; Miwa et al., 2013). The *ProBOR1:BOR1-GFP*, *ProBOR2:BOR2-GFP*, and *ProPIN2:PIN2-GFP* (Xu and Scheres, 2005) transgenes were introduced into the *ap2* mutants by crossing. The transgenic plants harboring *ProBRI1:BRI1-GFP* or *Pro-35S:GFP* were described previously (Ohkama et al., 2002; Geldner et al., 2007). Plants were grown in growth chambers (NK System; Nippon Medical and Chemical Instruments) with the following environmental parameters: 16-h/8-h light/dark cycle and 22°C under fluorescent lamps. Low-B medium (modified MGRL medium; Takano et al., 2005) containing 0.5 μM boric acid, 1% (w/v) Suc, and 1.5% (w/v) gellan gum (Wako Pure Chemicals) was used as standard plant growth medium.

Confocal Microscopy

For imaging analysis, plants were grown on low-B medium for 4 or 5 d. Confocal image acquisition was performed using a Leica TCS SP8 system equipped with a DMI6000B inverted microscope and two HyD hybrid detectors using ×40 water-immersion (numerical aperture = 1.10) and ×63 glycerol-immersion (numerical aperture = 1.30) objective lenses (Leica Microsystems). Laser excitations/spectral detection bandwidths were 488/500 to 530 nm for GFP, 488/650 to 700 nm for FM4-64, 488/650 to 750 nm for chlorophyll autofluorescence, and 561/570 to 650 nm for CF568. Image contrast was adjusted using the ImageJ and Fiji software (Schindelin et al., 2012). For orthogonal analysis of the cotyledon epidermis, *z* slices with 1-μm step size were obtained and reconstructed by the Orthogonal View algorithm in the Fiji software.

Drug Treatments

For FM4-64 staining, plants were incubated for 30 min in low-B liquid medium containing 1 μM FM4-64 (Thermo Fisher Scientific; 1 mM stock solution,

dissolved in water) and then washed twice with low-B liquid medium without FM4-64. For the BFA treatment, plants were treated with low-B liquid medium containing 50 μM cycloheximide (Wako Pure Chemicals; 25 mM stock solution, dissolved in water) for 30 min and then with 50 μM cycloheximide and 50 μM BFA for 60 min (Sigma-Aldrich; 50 mM stock solution, dissolved in dimethyl sulfoxide).

Confocal Image Quantification

The polarity index of BOR1-GFP in epidermal cells of root meristematic and transition zones was calculated as described previously (Yoshinari et al., 2016). The total signal in the inner half of the plasma membrane domain was divided by that in the outer half. Average data values from the apical and basal domains were used as the polarity index of each cell. The endocytic rate of BOR1-GFP was estimated by the following calculation: the average intensity of the intracellular GFP signal was divided by the average intensity of GFP signals in the apical and basal domains of the plasma membrane. To quantify BOR1-GFP signals in the plasma membrane after high-B supply, fluorescence intensities in the apical and basal plasma membrane domains in the epidermal cells were measured in each root.

Immunofluorescence Microscopy

Four-day-old seedlings grown on low-B medium containing 0.5 μM boric acid were used for immunofluorescence microscopy. Seedlings were fixed by 4% (w/v) paraformaldehyde diluted in MTSB buffer (50 mM PIPES, 5 mM EGTA, and 5 mM $MgSO_4$, pH 7.2) with 0.1% (v/v) Triton X-100 for 1 h at room temperature. Plant specimens were washed four times with MTSB buffer and twice with ultra-pure water. The specimens were dried on the slide glass for one night, rehydrated with MTSB buffer for 5 min, and then incubated with 2% (w/v) Driselase (Kyowa Hakko Kogyo) solution for 30 min at 37°C to digest the cell wall. After washing four times with MTSB buffer, the specimens were incubated with permeabilization buffer (MTSB buffer containing 3% [v/v] Nonidet P-40 [Nacalai Tesque] and 10% [v/v] dimethyl sulfoxide) for 60 min at room temperature. After washing five times with MTSB buffer, the specimens were incubated in blocking buffer (MTSB buffer containing 3% [w/v] BSA) for 1 h at room temperature. Then the specimens were incubated with the primary antibody (chicken anti-PIN2 antibody [1:1,000; Agrisera] diluted in the blocking buffer) for 4 h at 37°C and then for one night at 4°C. The specimens were washed six times with MTSB buffer and treated with the secondary antibody (goat anti-chicken IgY antibody conjugated with CF568 [1:250; Biotium]) for 3 h at 37°C. Then the specimens were washed six times with 250 μL of MTSB buffer and four times with ultra-pure water (milliQ; Merck Millipore) and were mounted with ProLong Diamond antifade solution (Thermo Fisher Scientific).

Preparation of Microsomal Proteins

For western-blot analysis of endogenous BOR1, total proteins were extracted from 2-week-old plants grown on low-B medium. The roots were homogenized in a homogenization buffer (250 mM Tris-HCl [pH 8.5], 290 mM Suc, 25 mM EDTA, 75 mM 2-mercaptoethanol, 0.5 mg mL^{-1} Pefabloc SC [Sigma-Aldrich; 50 mg mL^{-1} stock solution, dissolved in water], and one tablet/10 mL cOmplete Ultra Tablets, Mini, EDTA-free, Protease Inhibitor Cocktail [Roche]) using a Multibeads Shocker (Yasui Kikai). Cell debris was removed by centrifugation for 15 min at 15,000*g* at 4°C. Then microsomes were precipitated from the supernatant by ultracentrifugation for 30 min at 100,000*g* at 4°C. Microsomes were resuspended in 30 μL of storage buffer (50 mM KPi buffer [pH 6.3], 1 mM $MgSO_4$, 20% [v/v] glycerol, 0.5 mg mL^{-1} Pefabloc SC, and one tablet/10 mL cOmplete Ultra Tablets, Mini, EDTA-free, Protease Inhibitor Cocktail) and stored at −30°C.

Co-IP

For protein extraction, plants were grown on solid low-B medium for 2 weeks. Both the shoots and the roots were frozen in liquid nitrogen and ground by a Multibeads Shocker (Yasui Kikai). The ground tissues were homogenized with lysis buffer (25 mM Tris-HCl [pH 7.5], 50 mM NaCl, 10% [v/v] glycerol, 5 mM DTT, 1 mM Na_2MoO_4, 1 mM NaF, 1.5 mM Na_3VO_4, one tablet/50 mL cOmplete ULTRA Tablets [Roche], 2% [v/v] Nonidet P-40, and 0.25 mg mL^{-1} Pefabloc SC) by a Multibeads Shocker. Cell debris was removed by centrifugation for 15 min at 15,000*g* at 4°C.

Immunoaffinity complexes were isolated from the lysates using anti-GFP microbeads of the μMACS Epitope Tag Protein Isolation Kit (Miltenyi Biotec). The anti-GFP microbeads were incubated in the lysates for 30 min with rotation at 4°C. The lysate-microbeads mixtures were applied to columns, and the columns were washed three times with the lysis buffer. Then the immunoaffinity complexes were eluted with preheated elution buffer (50 mM Tris-HCl [pH 6.8], 1% [w/v] SDS, 0.005% [w/v] Bromophenol Blue, 10% [v/v] glycerol, and 100 mM DTT, 98°C).

Western-Blot Analysis

Proteins were loaded on NuPAGE 4-12% Bis-Tris Protein Gels (Thermo Fisher Scientific) and transferred to an Immobilon-P polyvinylidene difluoride membrane (pore size 0.45 μm; Merck Millipore) by a wet transfer technique. Rabbit anti-AP2A polyclonal antibody (1:2,000; Kim et al., 2013), mouse anti-GFP monoclonal antibody (1:8,000; Nacalai Tesque), and rabbit anti-BOR1 polyclonal antibody (1:2,000; Aibara et al., 2018) were diluted in Can Get Signal Solution 1 (Toyobo) and used as primary antibodies. Anti-rabbit or anti-mouse IgG antibody conjugated with horseradish peroxidase (GE Healthcare) was used at a 1:100,000 dilution in Can Get Signal Solution 2 (Toyobo) as secondary antibody. The membrane-bound proteins were stained with 0.25% (w/v) Coomassie Brilliant BlueR-250 after the detection.

Y2H Assay

Bait and prey vectors were cointroduced into the Y2H Gold yeast strain (Takara Clontech) as follows. Yeast cells grown overnight in yeast extract peptone dextrose liquid medium were washed and suspended in the One Step solution (40% polyethylene glycol, 200 mM lithium acetate, 100 mM DTT, 1 mM EDTA, and 10 mM Tris-HCl [pH 7.5]; modified after Chen et al., 1992). Carrier DNA (salmon sperm DNA; 1 mg mL^{-1} final concentration) and plasmid DNA (~15 μg mL^{-1} final concentration) were added, and the cells were incubated at 42°C for 1 h. The yeast suspensions were diluted 4-fold and spread onto synthetic complete (SC)-Leu-Trp double dropout medium. The plates were incubated for 3 d at 30°C.

For the two-hybrid assay, yeast transformants were preincubated overnight in SC liquid medium without Leu and Trp. The yeast cultures were diluted to OD_{600} = 0.2, 0.02, and 0.002 with sterilized water, and 10 μL was spotted onto SC-Leu-Trp double dropout or SC-Leu-Trp-His triple dropout medium. The plates were incubated for 3 d at 30°C. We used the control bait p53 and prey SV40 T-antigen supplied with the kit, Matchmaker Gold Yeast Two-Hybrid System (Takara Clontech).

Quantification of Root Length

The primary root lengths of 10-d-old seedlings were quantified using the segmented line tool of Fiji software.

Statistical Analyses

Statistical analyses in Figures 2 and 5 were performed using R (version 3.2.1) in an R studio environment (version 0.99.467). One-way ANOVA with a Steel-Dwass posthoc test was employed to determine statistically significant differences in the fluorescence ratio of GFP in cytoplasm and plasma membrane (Fig. 2B). Two-way ANOVA was employed to determine statistically significant differences in the relative GFP fluorescence levels in the plasma membrane of the epidermis after high-B supply (Fig. 5B). A two-tailed Student's *t* test was performed with a function in Microsoft Excel (version 16.16.6) for statistical analysis of the polarity index (Fig. 1B) and relative root length (Fig. 6C). Bar graphs show means ± SD.

Accession Numbers

Sequence data from this article can be found in the GenBank/EMBL data libraries under the following accession numbers: *BOR1* (AT2G47160), *BOR2* (AT3G62270), *AP1M2* (AT1G60780), *AP2M* (AT5G46630), *AP2S* (AT1G47830), *AP3M* (AT1G56590), *AP4M* (AT4G24550), *BRI1* (AT4G39400), *PIN2* (AT5G57090), and *TfR* (X01060).

Supplemental Data

The following supplemental materials are available.

Supplemental Figure S1. Subcellular localization of BOR1-GFP in the cotyledon epidermis of wild-type (*bor1-1*), *ap2m-2*, and *ap2s* plants.

Supplemental Figure S2. Polar localization of BOR2 and PIN2 in mutants of *AP2M* or *AP2S*.

Supplemental Figure S3. Y2H assay between the TfR and μ-subunits of Arabidopsis AP complexes.

Supplemental Figure S4. Specificity of the anti-BOR1 antibody.

Supplemental Figure S5. Vegetative growth of wild-type (Col-0), *bor1-3 bor2-1*, *ap2s*, and *ap2m-2* plants under a low-B condition.

Supplemental Table S1. Primers used in this research.

ACKNOWLEDGMENTS

We thank Tomoko Shimizu (Hokkaido University) for skillful technical assistance and Koh Aoki (Osaka Prefecture University) for guidance on the chemiluminescence detector. We are grateful to Christian Luschnig (University of Natural Resources and Life Sciences, Vienna) for providing us with PIN2-GFP seeds, Inhwan Huang (Pohang University of Science and Technology) for *ap2m-1* seeds and anti-AP2A antibody, Taiho Kambe (Kyoto University) for a human cDNA pool, and Joanne Chory (Salk Institute for Biological Studies) for BRI1-GFP seeds.

Received August 17, 2018; accepted January 24, 2019; published February 1, 2019.

LITERATURE CITED

Aibara I, Hirai T, Kasai K, Takano J, Onouchi H, Naito S, Fujiwara T, Miwa K (2018) Boron-dependent translational suppression of the borate exporter BOR1 contributes to the avoidance of boron toxicity. Plant Physiol **177:** 759–774

Alassimone J, Naseer S, Geldner N (2010) A developmental framework for endodermal differentiation and polarity. Proc Natl Acad Sci USA **107:** 5214–5219

Bashline L, Li S, Anderson CT, Lei L, Gu Y (2013) The endocytosis of cellulose synthase in Arabidopsis is dependent on μ2, a clathrin-mediated endocytosis adaptin. Plant Physiol **163:** 150–160

Bashline L, Li S, Zhu X, Gu Y (2015) The TWD40-2 protein and the AP2 complex cooperate in the clathrin-mediated endocytosis of cellulose synthase to regulate cellulose biosynthesis. Proc Natl Acad Sci USA **112:** 12870–12875

Chen DC, Yang BC, Kuo TT (1992) One-step transformation of yeast in stationary phase. Curr Genet **21:** 83–84

Dhonukshe P, Baluška F, Schlicht M, Hlavacka A, Šamaj J, Friml J, Gadella TWJ Jr (2006) Endocytosis of cell surface material mediates cell plate formation during plant cytokinesis. Dev Cell **10:** 137–150

Di Rubbo S, Irani NG, Kim SY, Xu ZY, Gadeyne A, Dejonghe W, Vanhoutte I, Persiau G, Eeckhout D, Simon S, et al (2013) The clathrin adaptor complex AP-2 mediates endocytosis of brassinosteroid insensitive1 in Arabidopsis. Plant Cell **25:** 2986–2997

Fan L, Hao H, Xue Y, Zhang L, Song K, Ding Z, Botella MA, Wang H, Lin J (2013) Dynamic analysis of Arabidopsis AP2 σ subunit reveals a key role in clathrin-mediated endocytosis and plant development. Development **140:** 3826–3837

Feraru E, Paciorek T, Feraru MI, Zwiewka M, De Groodt R, De Rycke R, Kleine-Vehn J, Friml J (2010) The AP-3 β adaptin mediates the biogenesis and function of lytic vacuoles in Arabidopsis. Plant Cell **22:** 2812–2824

Fuji K, Shirakawa M, Shimono Y, Kunieda T, Fukao Y, Koumoto Y, Takahashi H, Hara-Nishimura I, Shimada T (2016) The adaptor complex AP-4 regulates vacuolar protein sorting at the trans-Golgi network by interacting with VACUOLAR SORTING RECEPTOR1. Plant Physiol **170:** 211–219

Fujimoto M, Arimura S, Ueda T, Takanashi H, Hayashi Y, Nakano A, Tsutsumi N (2010) Arabidopsis dynamin-related proteins DRP2B and DRP1A participate together in clathrin-coated vesicle formation during endocytosis. Proc Natl Acad Sci USA **107:** 6094–6099

Funakawa H, Miwa K (2015) Synthesis of borate cross-linked rhamnogalacturonan II. Front Plant Sci **6:** 223

Gadeyne A, Sánchez-Rodríguez C, Vanneste S, Di Rubbo S, Zauber H, Vanneste K, Van Leene J, De Winne N, Eeckhout D, Persiau G, et al (2014) The TPLATE adaptor complex drives clathrin-mediated endocytosis in plants. Cell **156:** 691–704

Geldner N, Hyman DL, Wang X, Schumacher K, Chory J, (2007) Endosomal signaling of plant steroid receptor kinase BRI1. Genes Dev **21:** 1598–1602

Gu M, Liu Q, Watanabe S, Sun L, Hollopeter G, Grant BD, Jorgensen EM (2013) AP2 hemicomplexes contribute independently to synaptic vesicle endocytosis. eLife **2:** e00190

Hosy E, Martinière A, Choquet D, Maurel C, Luu DT (2015) Super-resolved and dynamic imaging of membrane proteins in plant cells reveal contrasting kinetic profiles and multiple confinement mechanisms. Mol Plant **8:** 339–342

Ito E, Fujimoto M, Ebine K, Uemura T, Ueda T, Nakano A (2012) Dynamic behavior of clathrin in Arabidopsis thaliana unveiled by live imaging. Plant J **69:** 204–216

Kaksonen M, Roux A (2018) Mechanisms of clathrin-mediated endocytosis. Nat Rev Mol Cell Biol **19:** 313–326

Kasai K, Takano J, Miwa K, Toyoda A, Fujiwara T (2011) High boron-induced ubiquitination regulates vacuolar sorting of the BOR1 borate transporter in Arabidopsis thaliana. J Biol Chem **286:** 6175–6183

Kim SY, Xu ZY, Song K, Kim DH, Kang H, Reichardt I, Sohn EJ, Friml J, Juergens G, Hwang I (2013) Adaptor protein complex 2-mediated endocytosis is crucial for male reproductive organ development in *Arabidopsis*. Plant Cell **25:** 2970–2985

Korbei B, Moulinier-Anzola J, De-Araujo L, Lucyshyn D, Retzer K, Khan MA, Luschnig C (2013) Arabidopsis TOL proteins act as gatekeepers for vacuolar sorting of PIN2 plasma membrane protein. Curr Biol **23:** 2500–2505

Li X, Pan SQ (2017) *Agrobacterium* delivers VirE2 protein into host cells via clathrin-mediated endocytosis. Sci Adv **3:** e1601528

Luschnig C, Vert G (2014) The dynamics of plant plasma membrane proteins: PINs and beyond. Development **141:** 2924–2938

Martinière A, Lavagi I, Nageswaran G, Rolfe DJ, Maneta-Peyret L, Luu DT, Botchway SW, Webb SE, Mongrand S, Maurel C, et al (2012) Cell wall constrains lateral diffusion of plant plasma-membrane proteins. Proc Natl Acad Sci USA **109:** 12805–12810

McMichael CM, Reynolds GD, Koch LM, Wang C, Jiang N, Nadeau J, Sack FD, Gelderman MB, Pan J, Bednarek SY (2013) Mediation of clathrin-dependent trafficking during cytokinesis and cell expansion by Arabidopsis stomatal cytokinesis defective proteins. Plant Cell **25:** 3910–3925

Mitsunari T, Nakatsu F, Shioda N, Love PE, Grinberg A, Bonifacino JS, Ohno H (2005) Clathrin adaptor AP-2 is essential for early embryonal development. Mol Cell Biol **25:** 9318–9323

Miwa K, Wakuta S, Takada S, Ide K, Takano J, Naito S, Omori H, Matsunaga T, Fujiwara T (2013) Roles of BOR2, a boron exporter, in cross linking of rhamnogalacturonan II and root elongation under boron limitation in Arabidopsis. Plant Physiol **163:** 1699–1709

Motley A, Bright NA, Seaman MN, Robinson MS (2003) Clathrin-mediated endocytosis in AP-2-depleted cells. J Cell Biol **162:** 909–918

Nagel MK, Kalinowska K, Vogel K, Reynolds GD, Wu Z, Anzenberger F, Ichikawa M, Tsutsumi C, Sato MH, Kuster B, et al (2017) *Arabidopsis* SH3P2 is an ubiquitin-binding protein that functions together with ESCRT-I and the deubiquitylating enzyme AMSH3. Proc Natl Acad Sci USA **114:** E7197–E7204

Ohkama N, Goto DB, Fujiwara T, Naito S (2002) Differential tissue-specific response to sulfate and methionine of a soybean seed storage protein promoter region in transgenic *Arabidopsis*. Plant Cell Physiol **43:** 1266–1275

Ohno H, Stewart J, Fournier MC, Bosshart H, Rhee I, Miyatake S, Saito T, Gallusser A, Kirchhausen T, Bonifacino JS (1995) Interaction of tyrosine-based sorting signals with clathrin-associated proteins. Science **269:** 1872–1875

Park M, Song K, Reichardt I, Kim H, Mayer U, Stierhof YD, Hwang I, Jürgens G (2013) Arabidopsis μ-adaptin subunit AP1M of adaptor protein complex 1 mediates late secretory and vacuolar traffic and is required for growth. Proc Natl Acad Sci USA **110:** 10318–10323

Richter S, Kientz M, Brumm S, Nielsen ME, Park M, Gavidia R, Krause C, Voss U, Beckmann H, Mayer U, et al (2014) Delivery of endocytosed proteins to the cell-division plane requires change of pathway from recycling to secretion. eLife **3:** e02131

Rossignol P, Collier S, Bush M, Shaw P, Doonan JH (2007) *Arabidopsis* POT1A interacts with TERT-V(I8), an N-terminal splicing variant of telomerase. J Cell Sci **120:** 3678–3687

Sancho-Andrés G, Soriano-Ortega E, Gao C, Bernabé-Orts JM, Narasimhan M, Müller AO, Tejos R, Jiang L, Friml J, Aniento F, et al (2016) Sorting motifs involved in the trafficking and localization of the PIN1 auxin efflux carrier. Plant Physiol **171:** 1965–1982

Sauer M, Delgadillo MO, Zouhar J, Reynolds GD, Pennington JG, Jiang L, Liljegren SJ, Stierhof YD, De Jaeger G, Otegui MS, et al (2013) MTV1 and MTV4 encode plant-specific ENTH and ARF GAP proteins that mediate clathrin-dependent trafficking of vacuolar cargo from the trans-Golgi network. Plant Cell **25:** 2217–2235

Schindelin J, Arganda-Carreras I, Frise E, Kaynig V, Longair M, Pietzsch T, Preibisch S, Rueden C, Saalfeld S, Schmid B, et al (2012) Fiji: An open-source platform for biological-image analysis. Nat Methods **9:** 676–682

Takano J, Noguchi K, Yasumori M, Kobayashi M, Gajdos Z, Miwa K, Hayashi H, Yoneyama T, Fujiwara T (2002) Arabidopsis boron transporter for xylem loading. Nature **420:** 337–340

Takano J, Miwa K, Yuan L, von Wirén N, Fujiwara T (2005) Endocytosis and degradation of BOR1, a boron transporter of *Arabidopsis thaliana*, regulated by boron availability. Proc Natl Acad Sci USA **102:** 12276–12281

Takano J, Tanaka M, Toyoda A, Miwa K, Kasai K, Fuji K, Onouchi H, Naito S, Fujiwara T (2010) Polar localization and degradation of Arabidopsis boron transporters through distinct trafficking pathways. Proc Natl Acad Sci USA **107:** 5220–5225

Teh OK, Shimono Y, Shirakawa M, Fukao Y, Tamura K, Shimada T, Hara-Nishimura I (2013) The AP-1 μ adaptin is required for KNOLLE localization at the cell plate to mediate cytokinesis in Arabidopsis. Plant Cell Physiol **54:** 838–847

Thurtle-Schmidt BH, Stroud RM (2016) Structure of Bor1 supports an elevator transport mechanism for SLC4 anion exchangers. Proc Natl Acad Sci USA **113:** 10542–10546

Traub LM (2009) Tickets to ride: Selecting cargo for clathrin-regulated internalization. Nat Rev Mol Cell Biol **10:** 583–596

Viotti C, Bubeck J, Stierhof YD, Krebs M, Langhans M, van den Berg W, van Dongen W, Richter S, Geldner N, Takano J, et al (2010) Endocytic and secretory traffic in *Arabidopsis* merge in the trans-Golgi network/early endosome, an independent and highly dynamic organelle. Plant Cell **22:** 1344–1357

Wang C, Hu T, Yan X, Meng T, Wang Y, Wang Q, Zhang X, Gu Y, Sánchez-Rodríguez C, Gadeyne A, et al (2016) Differential regulation of clathrin and its adaptor proteins during membrane recruitment for endocytosis. Plant Physiol **171:** 215–229

Wang JG, Li S, Zhao XY, Zhou LZ, Huang GQ, Feng C, Zhang Y (2013) HAPLESS13, the Arabidopsis μ1 adaptin, is essential for protein sorting at the trans-Golgi network/early endosome. Plant Physiol **162:** 1897–1910

Wang S, Yoshinari A, Shimada T, Hara-Nishimura I, Mitani-Ueno N, Feng Ma J, Naito S, Takano J (2017) Polar localization of the NIP5; 1 boric acid channel is maintained by endocytosis and facilitates boron transport in Arabidopsis roots. Plant Cell **29:** 824–842

Wang X, Cai Y, Wang H, Zeng Y, Zhuang X, Li B, Jiang L (2014) Trans-Golgi network-located AP1 gamma adaptins mediate dileucine motif-directed vacuolar targeting in Arabidopsis. Plant Cell **26:** 4102–4118

Wolfenstetter S, Wirsching P, Dotzauer D, Schneider S, Sauer N (2012) Routes to the tonoplast: The sorting of tonoplast transporters in *Arabidopsis* mesophyll protoplasts. Plant Cell **24:** 215–232

Xu J, Scheres B (2005) Dissection of Arabidopsis ADP-RIBOSYLATION FACTOR 1 function in epidermal cell polarity. Plant Cell **17:** 525–536

Yamaoka S, Shimono Y, Shirakawa M, Fukao Y, Kawase T, Hatsugai N, Tamura K, Shimada T, Hara-Nishimura I (2013) Identification and dynamics of Arabidopsis adaptor protein-2 complex and its involvement in floral organ development. Plant Cell **25:** 2958–2969

Yoshinari A, Takano J (2017) Insights into the mechanisms underlying boron homeostasis in plants. Front Plant Sci **8:** 1951

Yoshinari A, Kasai K, Fujiwara T, Naito S, Takano J (2012) Polar localization and endocytic degradation of a boron transporter, BOR1, is dependent on specific tyrosine residues. Plant Signal Behav **7:** 46–49

Yoshinari A, Fujimoto M, Ueda T, Inada N, Naito S, Takano J (2016) DRP1-dependent endocytosis is essential for polar localization and boron-induced degradation of the borate transporter BOR1 in *Arabidopsis thaliana*. Plant Cell Physiol **57:** 1985–2000

Yoshinari A, Korbei B, Takano J (2018) TOL proteins mediate vacuolar sorting of the borate transporter BOR1 in *Arabidopsis thaliana*. Soil Sci Plant Nutr **64:** 598–605

Zwiewka M, Feraru E, Möller B, Hwang I, Feraru MI, Kleine-Vehn J, Weijers D, Friml J (2011) The AP-3 adaptor complex is required for vacuolar function in Arabidopsis. Cell Res **21:** 1711–1722